Biogeosciences Discuss., 12, 19499–19534, 2015
www.biogeosciences-discuss.net/12/19499/2015/
doi:10.5194/bgd-12-19499-2015

Biogeosciences
Discussions
Open Access

Projecting the release of carbon from permafrost soils using a perturbed physics ensemble

A. H. MacDougall and R. Knutti

Institute for Atmospheric and Climate Science, ETH Zurich, Zurich, Switzerland

Received: 14 October 2015 – Accepted: 15 November 2015 – Published: 10 December 2015

Correspondence to: A. H. MacDougall (andrew.macdougall@env.ethz.ch)

Published by Copernicus Publications on behalf of the European Geosciences Union.

Abstract

The soils of the Northern Hemisphere permafrost region are estimated to contain 1100 to 1500 Pg of carbon (Pg C). A substantial fraction of this carbon has been frozen and therefore protected from microbial decay for millennia. As anthropogenic climate warming progresses much of this permafrost is expected to thaw. Here we conduct perturbed physics experiments on a climate model of intermediate complexity, with an improved permafrost carbon module, to estimate with formal uncertainty bounds the release of carbon from permafrost soils by year 2100 and 2300. We estimate that by 2100 the permafrost region may release between 56 (13 to 118) Pg C under Representative Concentration Pathway (RCP) 2.6 and 102 (27 to 199) Pg C under RCP 8.5, with substantially more to be released under each scenario by year 2300. A subset of 25 model variants were projected 8000 years into the future under continued RCP 4.5 and 8.5 forcing. Under the high forcing scenario the permafrost carbon pool decays away over several thousand years. Under the moderate scenario forcing a remnant near-surface permafrost region persists in the high Arctic which develops a large permafrost carbon pool, leading to global recovery of the pool beginning in mid third millennium of the common era (CE). Overall our simulations suggest that the permafrost carbon cycle feedback to climate change will make a significant but not cataclysmic contribution to climate change over the next centuries and millennia.

1 Introduction

Soils of the Northern Hemisphere permafrost region are estimated to contain between 1100 and 1500 Pg C of organic matter (Hugelius et al., 2014), roughly twice the quantity of carbon held in the pre-industrial atmosphere. As anthropogenic climate warming progresses, permafrost soils are expected to thaw exposing large quantities of organic matter to microbial decay, releasing CO_2 and CH_4 to the atmosphere (Schuur et al., 2015, 2008). Quantifying the strength and timing of this permafrost carbon cycle feedback to climate change has been a paramount goal of Earth system modelling in recent years (Zhuang et al., 2006; Koven et al., 2011, 2015; Schaefer et al., 2011; Schneider von Deimling et al., 2012; MacDougall et al., 2012; Burke et al., 2012, 2013; Schaphoff et al., 2013; Schneider von Deimling et al., 2015). However, large uncertainties in the physical and chemical properties of permafrost soils, as well as the simplified representation of permafrost processes in models have lead to a large spread in the projected release of carbon from permafrost soils (Schuur et al., 2015, for recent review). These model estimates range from 7 to 508 Pg C released from permafrost soils by year 2100 (Zhuang et al., 2006; MacDougall et al., 2012). New assessments of the size and susceptibility to decay of the permafrost carbon pool have recently become available (Hugelius et al., 2014; Schädel et al., 2014). These new studies are the first to formally quantify the uncertainty of permafrost carbon pool metrics based on field measurements and laboratory experiments. These new explicit constraints on uncertainty make it possible to propagate these uncertainties through models to place formal constrains on the release of carbon from permafrost soil.

For the purposes of analyzing incubation experiments and modelling of soil respiration, soil carbon is conventionally conceptualized as a small number of carbon pools each with an characteristic resistance to decay (e.g. Schmidt et al., 2011). A recent analysis of incubation experiments conducted with permafrost soils broke the permafrost carbon into a small (> 5 %) fast pool with and overturning time on the order of half a year, a moderate sized slow pool (∼ 5 to 60 %) with an overturning time on the order of a decade, and a large passive pool with and overturning time estimated at over a century to greater than 2500 years (Schädel et al., 2014). This multi-pool framework will be used to inform the modelling of the release of carbon from permafrost soils presented in this manuscript. However, we note that the physical and chemical basis of the multi-pool soil carbon conceptual model has been called into question by advances in soil science (Schmidt et al., 2011).

In general there are two sources of uncertainty in modelling: structural uncertainty and parameter uncertainty (Smith, 2007). Structural uncertainty arises from the discrepancy between the system that the model describes and the system the model is meant to represent in the natural world. Parameter uncertainty arises from uncertainty in the value of a model parameters. This can either be measurement uncertainty if the parameter is measurable in the natural world or more difficult to define when the parameter represents an amalgam of many physical phenomena (e.g. Smith, 2007). A third source of uncertainty distinctive to Earth system modelling (but not exclusively so) is scenario uncertainty. That is, uncertainty about how emission of CO_2 and other radiatively active substances will evolve in the future. This kind of uncertainty is conventionally dealt with by forcing a model with multiple future scenarios (e.g. Moss et al., 2010). Here our experiments will focus on parameter and scenario uncertainty, with a brief intercomparison to similar experiments with different models to acknowledge structural uncertainty.

There are many methods to propagate uncertainty in model parameters into uncertainty in model outputs (Helton and Davis, 2003). Of commonly used methods only the Montecarlo method and Latin hypercube sampling method do not require devising a statistical model of a physical model (Helton and Davis, 2003). In the Montecarlo method uncertain model parameters are selected randomly from their probability distribution functions and randomly paired with other selected parameter values to form parameter sets (Helton and Davis, 2003). This method is conceptually simple and easy to implement but many thousands of model simulations are needed to comprehensively sample parameter space (e.g. Steinacher et al., 2013). The Latin hypercube method was designed to approximate the Montecarlo method while using far fewer computational resources (McKay et al., 1979). In the Latin hypercube sampling method each probability distribution function is broken into intervals of equal probability. From each interval one parameter value is selected and matched randomly with other model parameter values selected in the same fashion to form parameter sets. In this method any number of model parameters can be perturbed without increasing the number of simulations. The number of required simulations is simply the number of intervals selected (McKay et al., 1979). The Latin hypercube sampling method has been shown to capture parameter sets of low probability but of high consequence, that other sampling methods can miss (McKay et al., 1979). Latin hypercube sampling was originally developed by engineers to assess the safety of nuclear power plants (McKay et al., 1979) but has been used to explore the effect of parameter uncertainty on projections of future climate change (e.g. Forest et al., 2002; Collins et al., 2007; Shiogama et al., 2012). Here we will propagate the newly quantified uncertainty in permafrost carbon parameter values through an improved version of the University of Victoria Earth System Climate Model (UVic ESCM) to quantify the uncertainty in the release of carbon from permafrost soils to the year 2300.

Muti-millennial simulations of anthropogenic climate change suggest that the temperature anomaly caused by the burning of fossil fuels will last over 100 000 years (Archer, 2005). Such simulations suggest that 10 000 years into the future global mean temperature will remain approximately two-thirds of its peak temperature anomaly above the pre-industrial mean (e.g. Eby et al., 2009). Much of the permafrost carbon pool is highly resistant to decay (Schädel et al., 2014), however the long lifetime of anthropogenic climate change implies that the pool will eventually decay and its carbon will be added to the ocean–atmosphere system. To explore the ultimate fate of the permafrost carbon pool we have extended a sub-selection of model simulations to common era year 10 000.

2 Methods

2.1 Model description

The UVic ESCM is a climate model of intermediate complexity with a full three dimensional ocean general circulation model coupled to a simplified moisture-energy balance atmosphere and thermodynamic-dynamic sea-ice model (Weaver et al., 2001). The model contains a full realization of the global carbon cycle. The terrestrial carbon cycle is simulated using the Top-down Representation of Interactive Foliage and Flora

Including Dynamics (TRIFFID) dynamic vegetation model. TRIFFID is composed of five plant function types: broadleaf trees, needleleaf trees, shrubs, C3 grasses, and C4 grasses. These plant function types compete with one-another for space in each grid cell based on the Lotka-Voterra equations (Cox et al., 2001). The simulated plants take up carbon through photosynthesis and distributed acquired carbon to plant growth and autotrophic respiration. Dead carbon is transferred to the soil carbon pool as litterfall and is distributed in the soil as an exponentially decreasing function of depth. The ocean inorganic carbon cycle is simulated following the protocols of the ocean carbon cycle model intercomparison project (Orr et al., 1999). Dissolved inorganic carbon is treated as a passive tracer by the model and carried throughout the ocean following ocean circulation (Weaver et al., 2001). Ocean biology is simulated using a nutrient-phytoplankton-zooplankton-detritus ocean biology scheme (Schmittner et al., 2008). The slow feedback between ocean alkalinity and calcite dissolution is simulated using an oxygen only representation of respiration of organic matter in sediments (Archer, 1996). The simplified atmospheric scheme makes it possible to alter the equilibrium climate sensitivity of the model (Zickfeld et al., 2008). This is accomplished by altering the outgoing longwave radiation to space as a function of global average near surface air temperature anomaly (Zickfeld et al., 2008).

The version of the UVic ESCM used here is based on the frozen ground version documented in Avis et al. (2011) and Avis (2012). This version of the model has a deep subsurface extending down to 250 m depth and is composed of 14 vertical layers. These layers are of unequal thickness and become exponentially thicker with depth. The top 8 layers (10 m) are hydraulically active and top 6 layers (3.35 m) are active in the carbon cycle. In the hydraulically active layers the subsurface porosity and permeability is prescribed based on the sand, silt, clay and organic matter content of the grid cell. These gridded data are interpolated from the International Satellite Land Surface Climate Project Initiative II (Scholes and de Colstoun, 2012). The model accounts for the effect of soil valence forces on freezing point and the fraction of frozen

Title Page
Abstract | Introduction
Conclusions | References
Tables | Figures
◀| |▶
◀ ▶
Back | Close
Full Screen / Esc
Printer-friendly Version
Interactive Discussion

and unfrozen water in soil is computed based on equations that minimize Gibbs free energy (Avis, 2012).

2.1.1 The permafrost carbon module

A permafrost carbon module was added to the UVic ESCM by MacDougall et al. (2012) and described in detail in MacDougall (2014). For the experiments conducted in this study the permafrost carbon module has been overhauled and improved. The permafrost carbon pool is now prognostically generated within the model using a diffusion scheme based on that of Koven et al. (2009). This scheme is meant to approximate the process of cryoturbation on the vertical distribution of soil carbon in permafrost affected soils. The scheme takes the form:

$$\frac{\partial C}{\partial t} = K_\mathrm{v} \frac{\partial^2 C_\mathrm{eff}}{\partial z^2}, \tag{1}$$

where C is the carbon concentration of the soil layer, t is time, z is the depth, K_v is the diffusion parameter, and C_eff is the effective carbon concentration of the layer. The diffusion parameter K_v is altered as a function of depth:

$$K_\mathrm{v} = \begin{cases} K_\mathrm{vo}, & \text{for} \quad z < z_\mathrm{ALT} \\ K_\mathrm{vo}\left(1 - \left(\frac{z - z_\mathrm{ALT}}{(k-1) z_\mathrm{ALT}}\right)\right), & \text{for} \quad z_\mathrm{ALT} < z < k z_\mathrm{ALT} \\ 0, & \text{for} \quad z > k z_\mathrm{ALT} \end{cases} \tag{2}$$

where K_vo is the cryoturbation mixing time scale, z_ALT is the thickness of the active layer, and k is a constant here taken as 4. The original scheme of Koven et al. (2009) has been modified for use in the UVic ESCM. A drawback of the original scheme is that it uses diminishing rate of diffusion with depth to produce the diminishing concentration of permafrost soil carbon with depth. This implies that the scheme must never be in equilibrium with the surface concentration of carbon to maintain this vertical carbon concentration gradient. When implemented this feature results in the size of the permafrost carbon pool being a function of the length of the model spin-up. From a model-design perspective this is a serious drawback as: (1) this will create a small model drift in atmospheric CO_2 concentration; and (2) in general the size of the permafrost carbon pool should not be a function of the time needed for the ocean carbonate chemistry to reach equilibrium.

To fix this deficiency, diffusion is carried out with an effective carbon concentration which is related to the actual carbon concentration by:

$$C_{\mathrm{eff}}(i) = \begin{cases} C, & \text{for} \quad i = 1 \\ C_{\mathrm{eff}} = \frac{C}{S\Theta}, & \text{for} \quad i > 1 \end{cases} \tag{3}$$

where i is the layer number, S is the saturation factor and Θ is the volumetric porosity of the layer. In the UVic ESCM the porosity of soil diminishes with depth and is a function of the sand, silt, clay fraction of the layer. The factor S was required to prevent permafrost soils from accumulating vastly more carbon than the estimated size of the permafrost carbon pool.

In the present version of the UVic ESCM permafrost carbon is treated as an entirely separate soil-carbon pool. Permafrost carbon is created when carbon is diffused across the permafrost table. The permafrost carbon can only be destroyed through simulated microbial respiration. This scheme allows the properties of the permafrost carbon to be prescribed. Permafrost carbon is also assigned an available fraction, which is effectively the combined fraction of the fast and slow soil carbon pools. When permafrost carbon decays the available fraction is reduced by the appropriate amount. The available fraction is increased as a function of time and soil temperature with a permafrost carbon transformation parameter determining the rate of change. This scheme effectively slowly transforms the passive fraction of the permafrost carbon into the slow soil carbon pool where it can be respired to CO_2. Described mathematically the scheme is:

$$R_{\mathrm{p}} = \kappa_{\mathrm{p}} C_{\mathrm{p}} A_f f_{\Theta} f_T \tag{4}$$

where R_p is permafrost carbon respiration, κ_p is the permafrost decay rate constant, C_p is the permafrost carbon density, f_Θ and f_T are respectively moisture and temperature dependent functions. A_f changes each time step:

$$A_f^{t+1} = C_\mathrm{p} A_f^t - R_\mathrm{p} + (\kappa_\mathrm{tf} C_p (1 - A_f^t) f_\Theta f_T), \quad (5)$$

where κ_tf is the rate constant for the transformation of carbon in the passive carbon pool into the slow carbon pool. Using this scheme the model can represent the large fraction of permafrost carbon that is in the passive carbon pool, while still allowing this passive pool to eventually decay.

2.2 Comparison to data

Figure 1 displays maps of the estimated soil carbon density in the top 3 m of soil in the Northern Hemisphere permafrost region as presented in Hugelius et al. (2014), compared to simulated soil carbon density in the top 3.35 m of the permafrost region as simulated by the UVic ESCM (using standard model parameter values). The maps show that the UVic ESCM generally simulates reasonable values for the density of carbon in the permafrost region but with substantial spatial biases. The model has too much carbon in northern fraction of the Fennoscandia peninsula, southern Alaska and near the Lena river basin. The model does not capture the large permafrost carbon density in the Hudson Bay lowlands and permafrost (and therefore permafrost carbon) is absent from the Labrador peninsula. However the model is able to capture some of the geographic features of the permafrost carbon pool including the high carbon density in northwestern Russia and the low carbon density in the eastern Canadian Arctic and Arctic archipelago.

The saturation factor from Eq. (3) was used to tune the total amount of carbon in the permafrost region such that in the default version of the model it matches the total from Hugelius et al. (2014) very closely. Therefore in year 1995 the simulated permafrost region has 1035 Pg C in the to 3.35 m, equal to the best estimate for the carbon in the top 3 m of permafrost soil provided by Hugelius et al. (2014). Carbon held in perennially frozen soil layers makes up 49 % of the carbon in the permafrost region in the UVic ESCM. This metric, which was not tuned, is very close to the estimate of ∼ 50 % provided by Hugelius et al. (2014).

2.3 Experiment design

We have chosen to perturb four parameters that describe the permafrost carbon pool: (1) the quantity of soil carbon in the top 3 m of soil in the permafrost region, taken from Hugelius et al. (2014). (2) The permafrost decay rate constant κ_p, computed from mean residence time of the slow permafrost soil carbon pool from Schädel et al. (2014). (3) The available fraction of permafrost carbon computed from the combined size of the fast and slow soil carbon pools in measured permafrost soils samples from Schädel et al. (2014). (4) The passive pool transformation rate κ_tf, estimated from Trumbore (2000). We also perturb two physical climate parameters: the climate sensitivity and the arctic amplification factor.

The quantity of carbon in permafrost soils is controlled by changing the saturation factor S presented in Eq. (3). Calibration simulations were conducted with the UVic ESCM to derive a functional relationship between S and the quantity of carbon in permafrost soils. The Probability Distribution Function (PDF) for the permafrost carbon quantity (in the top 3 m of soil) was taken as a normal distribution with a mean of 1035 Pg C and a standard deviation of 75 Pg C, taken from Hugelius et al. (2014). The permafrost carbon decay rate is derived from the mean residence time of the slow carbon pool in permafrost soils. The permafrost decay rate is taken to be normally distributed with a mean of 7.45 years and a standard deviation of 2.67 years, with values taken form Schädel et al. (2014). The available fraction is described by the sum of three weighted gamma distributions with each distribution respectively describing the PDF of the organic, shallow mineral (< 1 m), and deep mineral (> 1) soils. The weights for the PDFs were derived from the relative fraction of permafrost soil carbon in organic, shallow mineral and deep mineral soils from Hugelius et al. (2014). The parameter values for the PDFs were derived by fitting gamma functions to the data in Fig. 3 of Schädel et al. (2014). The passive pool transformation rate is very poorly constrained as the incubation experiments analyzed by Schädel et al. (2014) were unable to constrain the parameter's value (the contribution from the passive carbon pool was too small to be detected). The value of the parameter was estimated from the ^{14}C age of the passive carbon pool from mid-latitude soils (Trumbore, 2000). The mean residence time at 5 °C was estimated at 300–5000 years with a best guess of 1250 years yielding a passive pool transformation rate of 0.25×10^{-10} to $4\times10^{-10}\,\mathrm{s}^{-1}$, with a best guess of $1\times10^{-10}\,\mathrm{s}^{-1}$. The PDF was taken as uniform in base-two log-space.

Arctic amplification can be changed in the UVic ESCM by changing the meridional diffusivity of the simplified atmospheric model (Fyke et al., 2014; Fyke, 2011). Here the Arctic amplification factor was taken to be normally distribution with a mean of 1.9 and standard deviation of 0.2 (Serreze and Barry, 2011). Many studies have attempted to derive a PDF of equilibrium climate sensitivity (Collins et al., 2013, for recent summary) from model based, observational and paleoclimate evidence. Here we chose to use a PDF that captures the general features of these distributions with a mean of 3.25 °C for doubling of CO_2 and the 5th and 95th percentile 1.7 and 5.2 °C respectively (Olson et al., 2012). The PDFs for all six perturbed parameters are shown in Fig. 2.

The Latin hypercube sampling, described in the introduction, was used to create the parameter sets. Each PDF was sampled from 25 equal-probability intervals and value selected from each interval was randomly matched to one of the values selected from each of the other PDFs to create a "cube" containing 25 parameter sets. This sampling was repeated ten times to create ten cubes for a total of 250 model variants. Each of these variants was spun-up for 5000 years under estimated year 1850 forcing to generate the permafrost carbon pool. Each model variant was forced with historical forcing followed by each of the four Representative Concentration Pathways (RCPs) used in the fifth assessment report of the Intergovernmental Panel on Climate Change (IPCC AR5). The simulations were carried out with prescribed atmospheric

CO_2 concentrations and compatible anthropogenic CO_2 emissions were diagnosed as a residual of the carbon cycle.

The old permafrost carbon capable version of the UVic ESCM was able to quantify the previously unaccounted for temperature effect of the permafrost carbon feedback by comparing model simulations with and without permafrost carbon (MacDougall et al., 2012). This has become much more difficult with the introduction of the permafrost carbon pool diffusion module. This soil carbon diffusion scheme causes the active layer to accumulate more soil carbon than in the model version without a prognostically generated permafrost soil carbon pool. Consequently we can no-longer easily “turn-off” the permafrost carbon. Therefore we have chosen to conduct experiments which quantify the permafrost carbon feedback in-terms of carbon released from permafrost affected soils. As carbon released from permafrost soil displaces fossil fuel carbon in the carbon budget (MacDougall et al., 2015) we feel this is the most policy-relevant metric.

Twenty-five model variants (one cube) was projected into the deep-future under continued RCP 4.5 and 8.5 forcing. For this experiment only the four permafrost carbon parameter were perturbed and climate sensitivity and arctic amplification were held at their model default values. For each scenario the models were forced with prescribed atmospheric CO_2 concentration until peak CO_2 concentration was reached (year 2150 for RCP 4.5 and year 2250 for RCP 8.5). Thereafter the simulated CO_2 emissions were set to zero and atmospheric CO_2 was allowed to freely evolve. All other RCP forcings follow their prescribed trajectory until year 2300 and subsequently are held constant. The simulations were continued until the year 10 000 CE. Expecting non-CO_2 forcings to be constant for thousands of years following year 2300 is highly idealized, however this was seen as the simplest approach for evaluating the long-term response of the permafrost carbon pool to anthropogenic forcing.

3 Results

3.1 Release of carbon to 2300

The release of carbon from permafrost soils for each RCP and for each of the 250 model variants is shown in Fig. 3. Model results in this section are quoted as the mean value of all model variants with the 5th and 95th percentile range in brackets. This is equivalent to the "very likely" range from IPCC AR5, although the numbers here are of course conditional on the model structure and parameter PDFs chosen. By year 2100 the model estimates that 56 (13 to 118) Pg C will be released under RCP 2.6, 71 (16 to 146) Pg C released under RCP 4.5, 74 (15 to 154) Pg C released under RCP 6.0, and 102 (27 to 199) Pg C released under RCP 8.5. By year 2300 the model estimates that 91 (32 to 175) Pg C will be released under RCP 2.6, 149 (45 to 285) Pg C released under RCP 4.5, 204 (63 to 371) Pg C released under RCP 6.0, and 376 (159 to 587) Pg C released under RCP 8.5. These results are generally consistent with the inter-model range of 37 to 174 Pg C, mean of 92 Pg C by year 2100 under RCP 8.5 from Schuur et al. (2015).

The emission rate of CO_2 from permafrost soils carbon is shown in Fig. 4. Peak emissions under RCP 2.6 is 0.56 (0.13 to 1.29) $\mathrm{Pg\,C\,a^{-1}}$, under RCP 4.5 is 0.66 (0.16 to 1.57) $\mathrm{Pg\,C\,a^{-1}}$, under RCP 6.0 is 0.75 (0.19 to 1.59) $\mathrm{Pg\,C\,a^{-1}}$, and under RCP 8.5 is 1.05 (0.28 to 2.36) $\mathrm{Pg\,C\,a^{-1}}$. The timing of peak emissions of CO_2 from permafrost soils varies by model variant and scenario followed (Fig. 4) but generally occurs in the mid to late 21st century or early 22nd century in the case of RCP 6.0. These simulated peak emissions rate are of similar magnitude to modern land use change emissions, $0.9 \pm 0.8\,\mathrm{Pg\,C\,a^{-1}}$ averaged over the 2000–2011 period (Ciais et al., 2013). Even in the most extreme bound emissions from permafrost carbon are projected to be far lower than modern CO_2 emissions from fossil fuel burning and cement production ($9.5 \pm 0.8\,\mathrm{Pg\,C\,a^{-1}}$ in 2011) (Ciais et al., 2013).

The permafrost carbon feedback's effect on climate change will ultimately be determined by how large the release of carbon from permafrost soils is relative to the cumulative fossil fuel emissions (MacDougall and Friedlingstein, 2015). This notion follows from the near-linear relationship between cumulative emissions of CO_2 and change in global temperature (Matthews et al., 2009; Gillett et al., 2013). A relationship which emerges from the interaction of atmospheric and oceanic processes, with the land surface source or sink effectively acting in the same manner as fossil fuel emissions (MacDougall and Friedlingstein, 2015). The release of carbon from permafrost soils relative to the diagnosed cumulative emissions for each model variant and RCP scenarios are shown in Fig. 5. The relative emissions are highest under RCP 2.6 where emissions from permafrost soil are 13 (2 to 39) % of fossil fuel emissions in 2100 and 21 (5 to 54) % of fossil fuel emissions by 2300. Under RCP 8.5 carbon released from permafrost soils is only 2 (0.5 to 5) % of fossil fuel emissions in 2100 and 8 (3 to 14) % of fossil fuel emission by 2300. RCPs 4.5 and 6.0 fall between these bounds with 7 (1 to 16) % and 4 (1 to 10) % by 2100 respectively, and 14 (3 to 29) % and 12 (3 to 24) % respectively by 2300. These results suggest the the permafrost carbon feedback to climate change will be a more important climate change feedback in scenarios with substantial mitigation, consistent with previous studies (e.g. MacDougall et al., 2012).

3.2 Parameter uncertainty

The relative importance of uncertainty from each perturbed model parameter to the overall uncertainty can be evaluated by computing the correlation coefficient between the parameter value and the value of some model output (e.g Shiogama et al., 2012). In Fig. 6 the correlation between each of the six perturbed model parameters and release of carbon from permafrost soils under RCP 8.5 by year 2100 is shown. This particular metric was chosen as it has become the benchmark to compare simulations of the permafrost carbon feedback (e.g. Schuur et al., 2015). The two highest correlations are for the initial available fraction with an R value of 0.78 and climate sensitivity with an R value of 0.51. Correlations for the other perturbed parameters are less than 0.13. These correlations suggest that reducing the uncertainty in the release of carbon from permafrost soils by 2100 requires better quantification of the size of the fast and slow carbon pools in permafrost soils. Also important is reducing the uncertainty in climate sensitivity, already a paramount if intractable problem in climate science (e.g. Collins et al., 2013; Knutti and Hegerl, 2008). The four other perturbed parameters are relatively unimportant for reducing uncertainty to year 2100.

Correlations were also conducted between each model perturbed parameter value and release of carbon from permafrost soils by year 2300. By 2300 the importance of the initial available fraction has decreased and has an R value of 0.36, the correlation with permafrost carbon transformation rate has increased to an R value of 0.43 and the correlation of with climate sensitivity has increased to 0.64. The correlations with initial quantity of carbon in the permafrost region, permafrost carbon decay rate, and arctic amplification remain weak in this time frame, at 0.13, 0.02, and 0.11 respectively. These results demonstrate that the relative importance of uncertainty in parameters changes depending on the time frame of interest.

The low sensitivity of the release of carbon from permafrost soils to the value of Arctic amplification appears counterintuitive. However, most of the carbon held in the permafrost region is held in the region's southern extent (Fig. 1), while Arctic amplification has the greatest effect over the Arctic ocean, Greenland Icesheet, and Canadian Arctic Archipelago where there is little simulated carbon permafrost carbon.

Overall these results are encouraging as the most important factor for determining release of carbon from permafrost soils in the next century, the size of the permafrost carbon fast and slow pools, can be measured with incubation experiments (e.g. Schädel et al., 2014). A major field campaign to collect samples of permafrost carbon and conduct incubation experiments could therefore significantly reduce uncertainty in the strength of the permafrost carbon feedback to climate change.

3.3 Temperature sensitivity of permafrost carbon release

Climate change mitigation targets are often framed in terms of some global temperature change threshold not to be breached (e.g. Knutti and Rogelj, 2015). Therefore examining the relationship between global temperate change and the release of carbon from permafrost soils is of interest. Figure 7 shows the correlation between change in global temperature and the release of carbon from the permafrost soils for all model variants and RCPs at years 2100, 2200 and 2300. The figure shows that there is a clear correlation between the two quantities at all three time horizons. However, the slope of the correlation evolves in time from 24 $\mathrm{Pg\,C\,K^{-1}}$ in 2100, to 39 $\mathrm{Pg\,C\,K^{-1}}$ in 2200, and 47 $\mathrm{Pg\,C\,K^{-1}}$ in 2300. These correlations demonstrate a key feature of the permafrost carbon system: the long time-lag between forcing and response. That is, if fossil fuel emissions are eliminated and global temperature stabilizes, permafrost soils are expected to continue to release carbon for a very long time.

3.4 The deep future

The evolution of global mean temperature and atmospheric CO_2 concentration for the deep future experiments are shown in Fig. 8. Under continued non-CO_2 RCP 4.5 forcing and with zero CO_2 emissions, CO_2 concentration falls until about the 28th century under all model variants, and thereafter drifts slowly up or down depending on model variant. Under this scenario temperature continues to increase following cessation of emissions, becomes relatively stable for several centuries, experiences a period of renewed rapid warming in the late third millennium CE then becomes stable thereafter. Under continued RCP 8.5 forcing atmospheric CO_2 declines monotonically after cessation of emissions, reaching concentration below 1600 ppm by year 10 000 CE. Temperature continues to slowly increase following cessation of emissions, reaching a peak in the fifth millennium CE. Thereafter, temperature begins a slow decline. The long-term evolution of temperature and atmospheric CO_2

shown in these experiments is somewhat different from that in Eby et al. (2009) which showed larger declines in temperature and atmospheric CO_2 for comparable cumulative emissions and timeframe. The continued existence of non-CO_2 forcing in these scenarios and the inclusion of the permafrost carbon module are probable causes of the differences between that study and the present study.

The response of the permafrost carbon pool to millennia of anthropogenically enhanced temperatures varies by scenario followed. Under RCP 8.5 the pool monotonically declines with time, with the rate of decline varying by parameter set (Fig. 9). By the year 10 000 CE most of the model variants asymptote toward a carbon pool of about 10 Pg C, held around the fringes of Antarctica. Under RCP 4.5 the permafrost carbon pool begins a recovery before the year 3000 CE (Fig. 9), with permafrost soil carbon reaching a nadir in the year 2411 (2254–2605) CE. Some of the parameter sets show renewed reduction in permafrost carbon about 2000 years after the recovery begins. The origin of this recovery, despite continued elevated global temperatures, is the creation of a large permafrost carbon pool in the Canadian Arctic archipelago and the high Russian Arctic as shown in Fig. 10. This region is thought to contain very little soil carbon in the modern climate (see Fig. 1), a feature of the system that is captured by the model (Fig. 1). Under this scenario these regions accumulate large permafrost carbon pools as they remain permafrost bound but with much higher net primary productivity from overlying vegetation. These simulations suggest that the ultimate fate of the permafrost carbon pool is highly contingent on scenario followed.

4 Discussion

The release of carbon in these simulations is smaller than the previous estimate using an earlier version of this model (MacDougall et al., 2012). That study estimated that release of carbon from permafrost soils of 174 (68 to 508) Pg C by 2100. The comparable range from this study is 102 (27 to 199) Pg C. The greatest difference between these two versions of the UVic ESCM is the treatment of the passive soil carbon fraction of the permafrost carbon pool. The recent analysis of Schädel et al. (2014) showed that the passive pool makes up a larger fraction of permafrost carbon than the few studies available in 2011 had suggested when the simulations of MacDougall et al. (2012) were performed. Incorporating this new data into the model has reduced the estimated released of carbon from permafrost soils by year 2100 by about half.

The study most similar to the present study is that of Schneider von Deimling et al. (2015) which used a complex box model of the permafrost carbon system to conduct perturbed physics ensemble simulations. That study estimated the release of carbon from thawed permafrost soil only, and does not compute the release of carbon from the historic active layer. Schneider von Deimling et al. (2015) estimates that under RCP 2.6 36 (20 to 58, 68 % range) Pg C will be released by 2100. The comparable 68 % range from the experiments conducted with the UVic ESCM (accounting only for release of permafrost carbon and not for carbon release from the historic active layer) is 46 (19 to 75, 68 % range) Pg C by 2100. Under RCP 8.5 Schneider von Deimling et al. (2015) estimated that 87 (42 to 141, 68 % range) Pg C would be released from thawed permafrost by 2100 compared to 75 (31 to 120, 68 % range) Pg C in the UVic ESCM. The study of Schneider von Deimling et al. (2015) and the present study use radically different modelling structures but converge on very similar estimates of the release of carbon from permafrost soil. This suggests that parameter uncertainty dominates the uncertainty in projecting the release of carbon from permafrost soils and that a perturbed parameter approach can successfully capture the uncertainty in the permafrost carbon model component. The inter-model range from a recent review paper on the permafrost carbon feedback (Schuur et al., 2015) was 92 (37 to 174) Pg C under RCP 8.5, which compares favourably the the 90 % range in the present study of 102 (27 to 199) Pg C. Overall it appears that modelling studies of release of carbon from permafrost soils are converging toward a common estimate of the strength of the feedback.

There are many processes that effect the thawing of permafrost and decay of permafrost carbon that the UVic ESCM does not account for. The UVic ESCM has permafrost carbon only in the top 3.35 m of soil and therefore does not account for the substantial quantity of carbon held below 3 m in deltaic deposits 91 ± 52 Pg C and the Yedoma region 181 ± 54 Pg C (Hugelius et al., 2014). Other modelling studies suggest that the contribution from these deep soil deposits will be small in the coming centuries (e.g. Schneider von Deimling et al., 2015) but this pool of carbon would likely affect the results of our deep-future experiments. The UVic ESCM accounts for only two of the four mechanisms of permafrost thaw: active-layer thickening and talik formation; and does not simulate thermokarst development or soil erosion. The UVic ESCM does not simulate the production of methane from thawed soils. As warming from methane is proportional to the rate of emissions and not cumulative emissions (e.g. Pierrehumbert, 2014) it is unlikely that plausible rates of emission of methane from thawed permafrost soils will contribute cataclysmically to climate change (e.g. Schuur et al., 2015). The global dynamic vegetation scheme used by the UVic ESCM does not account for the effect of nutrient limitations on plant growth. The decay of organic matter in permafrost soils releases nutrients into the soils which presumably should enhance plant growth (e.g. Schuur et al., 2008), representing an unaccounted for negative feedback.

The quantity of carbon held in the Northern Hemisphere permafrost region is enormous but incubation experiments conducted on samples of this organic matter show that most of it is highly resistant to decay (Schädel et al., 2014). Interpretation of these incubation experiments and models of soil carbon decay are usually based on the multi-pool soil carbon conceptual model that has been called into question by advances in soil science (Schmidt et al., 2011). Discovering the actual physical and chemical mechanisms that stabilize permafrost soil carbon and assessing whether these mechanisms will be maintained as high latitude ecosystems undergo radical change in the coming centuries is paramount for assessing the strength of the permafrost carbon cycle feedback. That these mechanisms remain poorly understood represents perhaps the greatest uncertainty in assessing the permafrost carbon feedback.

5 Conclusions

Here we have used a perturbed physic ensemble to place an uncertainty constraint on the release of carbon from permafrost soils. We find that by 2100 the permafrost region may release 56 (13 to 118) Pg C under RCP 2.6, 71 (16 to 146) Pg C under RCP 4.5, 74 (15 to 154) Pg C under RCP 6.0, and 102 (27 to 199) Pg C under RCP 8.5, with substantially more to be released under each scenario by 2300. Of the six parameters perturbed the simulations are most sensitive in year 2100 to uncertainty in the size of the non-passive soil carbon pools and the equilibrium climate sensitivity. Additionally, by 2300 the transformation rate of the passive pool into carbon susceptible to decayed has become important. The simulations are insensitive to uncertainty in Arctic amplification, slow carbon pool overturning time, and the initial quantity of carbon in the permafrost region. Our results suggest that a large field campaign combined with incubation experiments to better constrain the size of the fast and slow carbon pools in permafrost soils could substantially reduced the uncertainty in the strength of the permafrost carbon cycle feedback. Contingent on our model structure being reflective of the natural world.

We have also projected a subset of a model variants into the deep future, with simulations conducted to the year 10 000 CE under continued RCP 4.5 and 8.5 forcing. These simulations suggest that if permafrost survives in the high arctic that a new permafrost carbon pool may develop leading to a recovery of this carbon pool. Under higher forcing where near surface permafrost ceases to exist outside Antarctica, the permafrost carbon pool almost totally decays away over several thousand years. Overall our simulations suggest that the permafrost carbon cycle feedback to climate change will make a substantial but not cataclysmic contribution to climate change over the next centuries and millennia.

Acknowledgements. We are indebted to the efforts of the Permafrost Carbon Network for organizing the collection of data on permafrost carbon quantity and quality. G. Hugelius graciously provided the data for the map in Fig. 1. In particular we thank C. Schädel for providing additional data on the quality of permafrost carbon.

References

Archer, D.: A data-driven model of the global calcite lysocline, Global Biogeochem. Cy., 10, 511–526, 1996. 19504

Archer, D.: Fate of fossil fuel CO_2 in geologic time, J. Geophys. Res., 110, C09S05, doi:10.1029/2004JC002625, 2005. 19503

Avis, C. A.: Simulating the present-day and future distribution of permafrost in the UVic Earth system climate model, PhD thesis, University of Victoria, Canada, 2012. 19504, 19505

Avis, C. A., Weaver, A. J., and Meissner, K. J.: Reduction in areal extent of high–latitude wetlands in response to permafrost thaw, Nat. Geosci., 4, 444–448, doi:10.1038/ngeo1160, 2011. 19504

Burke, E. J., Hartley, I. P., and Jones, C. D.: Uncertainties in the global temperature change caused by carbon release from permafrost thawing, The Cryosphere, 6, 1063–1076, doi:10.5194/tc-6-1063-2012, 2012. 19501

Burke, E. J., Jones, C. D., and Koven, C. D.: Estimating the permafrost-carbon climate response in the CMIP5 climate models using a simplified approach, J. Climate, 26, 4897–4909, 2013. 19501

Ciais, P., Sabine, C., Bala, G., Bopp, L., Brovkin, V., Canadell, J., Chhabra, A., DeFries, R., Galloway, J., Heimann, M., Jones, C., Quéé, C. L., Myneni, R. B., Piao, S., and Thornton, P.: Carbon and other biogeochemical cycles, in: Working Group I Contribution to the Intergovernmental Panel on Climate Change Fifth Assessment Report Climate Change 2013: The Physical Science Basis, edited by: Stocker, T. F., Qin, D., Plattner, G.-K., Tignor, M., Allen, S. K., Boschung, J., Nauels, A., Xia, Y., Bex, V., and Midgley, P., Cambridge University Press, Cambridge United Kingdom and New York, NY, United States, 465–570, 2013. 19511

Collins, M., Brierley, C., MacVean, M., Booth, B., and Harris, G.: The sensitivity of the rate of transient climate change to ocean physics perturbations, J. Climate, 20, 2315–2320, 2007. 19503

Collins, M., Knutti, R., Arblaster, J. M., Dufresne, J.-L., Fichefet, T., Friedlingstein, P., Gao, X., Jr., W. J. G., Johns, T., Krinner, G., Shongwe, M., Tebaldi, C., Weaver, A. J., and Wehner, M.: Long-term climate change: projections, commitments and irreversibility, in: Working Group I Contribution to the Intergovernmental Panel on Climate Change Fifth Assessment Report Climate Change 2013: The Physical Science Basis, Cambridge University Press, Cambridge United Kingdom and New York, NY, United States, 1029–1136, 2013. 19509, 19513

Cox, P. M., Betts, R. A., Jones, C. D., Spall, S. A., and Totterdell, I. J.: Modelling vegetation and the carbon cycle as interactive elements of the climate system, Proceedings of the RMS Millennium Conference, Hadley Centre technical note 23, 29 pp., 2001. 19504

Eby, M., Zickfeld, K., Montenegro, A., Archer, D., Meissner, K. J., and Weaver, A. J.: Lifetime of anthropogenic climate change: millennial time scales of potential CO_2 and surface temperature perturbations, J. Climate, 22, 2501–2511, doi:10.1175/2008JCLI2554.1, 2009. 19503, 19515

Forest, C. E., Stone, P. H., Sokolov, A. P., Allen, M. R., and Webster, M. D.: Quantifying uncertainties in climate system properties with the use of recent climate observations, Science, 295, 113–117, 2002. 19503

Fyke, J., Eby, M., Mackintosh, A., and Weaver, A.: Impact of climate sensitivity and polar amplification on projections of Greenland Ice Sheet loss, Clim. Dynam., 43, 2249–2260, 2014. 19509

Fyke, J. G.: Simulation of the global coupled climate/ice sheet system over millennial timescales, PhD thesis, Victoria University of Wellington, Wellington, New Zealand, 2011. 19509

Gillett, N. P., Arora, V. K., Matthews, D., and Allen, M. R.: Constraining the ratio of global warming to cumulative CO_2 emissions using CMIP5 simulations, J. Climate, 26, 6844–6858, 2013. 19512

Helton, J. C. and Davis, F. J.: Latin hypercube sampling and the propagation of uncertainty in analyses of complex systems, Reliab. Eng. Syst. Safe., 81, 23–69, 2003. 19502

Hugelius, G., Strauss, J., Zubrzycki, S., Harden, J. W., Schuur, E. A. G., Ping, C.-L., Schirrmeister, L., Grosse, G., Michaelson, G. J., Koven, C. D., O'Donnell, J. A., Elberling, B., Mishra, U., Camill, P., Yu, Z., Palmtag, J., and Kuhry, P.: Estimated stocks of circumpolar permafrost carbon with quantified uncertainty ranges and identified data gaps, Biogeosciences, 11, 6573–6593, doi:10.5194/bg-11-6573-2014, 2014. 19500, 19501, 19507, 19508, 19517, 19525

Knutti, R. and Hegerl, G. C.: The equilibrium sensitivity of the Earth's temperature to radiation changes, Nat. Geosci., 1, 735–743, 2008. 19513

Knutti, R. and Rogelj, J.: The legacy of our CO_2 emissions: a clash of scientific facts, politics and ethics, Climatic Change, 133, 361–373, 2015. 19514

Koven, C., Friedlingstein, P., Ciais, P., Khvorostyanov, D., Krinner, G., and Tarnocai, C.: On the formation of high-latitude soil carbon stocks: Effects of cryoturbation and insulation by organic matter in a land surface model, Geophys. Res. Lett., 36, L21501, doi:10.1029/2009GL040150, 2009. 19505

Koven, C. D., Ringeval, B., Friedlingstein, P., Ciais, P., Cadule, P., Khvorostyanov, D., Krinner, G., and Tarnocai, C.: Permafrost carbon–climate feedbacks accelerate global warming, P. Natl. Acad. Sci. USA, 108, 14769–14774, doi:10.1073/pnas.1103910108, 2011. 19501

Koven, C. D., Schuur, E. A. G., Schädel, C., Bohn, T. J., Burke, E. J., Chen, G., Chen, X., Ciais, P., Grosse, G., Harden, J. W., Hayes, D. J. Hugelius, G., Jafarov, E. E., Krinner, G., Kuhry, P., Lawrence, D. M., MacDougall, A. H., Marchenko, S. S., McGuire, A. D., Natali, S. M., Nicolsky, D. J. Olefeldt, D., Peng, S., Romanovsky, V. E., Schaefer, K. M., Strauss, J., Treat, C. C., and Turetsky, M.: A simplified, data-constrained approach to estimate the permafrost carbon–climate feedback, Phil. Trans. R. Soc. A, 373, 20140423, doi:10.1098/rsta.2014.0423, 2015. 19501

MacDougall, A.: A modelling study of the permafrost carbon feedback to climate change: feedback strength, timing, and carbon cycle consequences, PhD thesis, University of Victoria, Canada, 2014. 19505

MacDougall, A. H. and Friedlingstein, P.: The origin and limits of the near proportionality between climate warming and cumulative CO_2 emissions, J. Climate, 28, 4217–4230, doi:10.1175/JCLI-D-14-00036.1, 2015. 19512

MacDougall, A. H., Avis, C. A., and Weaver, A. J.: Significant existing commitment to warming from the permafrost carbon feedback, Nat. Geosci., 5, 719–721, doi:10.1038/NGEO1573, 2012. 19501, 19505, 19510, 19512, 19515, 19516

MacDougall, A. H., Zickfeld, K., Knutti, R., and Matthews, H. D.: Sensitivity of carbon budgets to permafrost carbon feedbacks and non-CO_2 forcings, Environ. Res. Lett., 10, 125003, doi:10.1088/1748-9326/10/12/125003, 2015. 19510

Matthews, H. D., Gillett, N. P., Stott, P. A., and Zickfeld, K.: The proportionality of global warming to cumulative carbon emissions, Nature, 459, 829–832, doi:10.1038/nature08047, 2009. 19512

McKay, M. D., Beckman, R. J., and Conover, W. J.: Comparison of three methods for selecting values of input variables in the analysis of output from a computer code, Technometrics, 21, 239–245, 1979. 19502, 19503

Moss, R. H., Edmonds, J. A., Hibbard, K. A., Manning, M. R., Rose, S. K., van Vuuren, D. P., Carter, T. R., Emori, S., Kainuma, M., Kram, T., Meehl, G. A., Mitchell, J. F. B., Nakicenovic, N., Riahi, K., Smith, S. J., Stouffer, R. J., Thomson, A. M., Weyant, J. P., and Wilbanks, T. J.: The next generation of scenarios for climate change research and assessment, Nature, 463, 747–754, doi:10.1038/nature08823, 2010. 19502

Olson, R., Sriver, R., Goes, M., Urban, N. M., Matthews, H. D., Haran, M., and Keller, K.: A climate sensitivity estimate using Bayesian fusion of instrumental observations and an Earth System model, J. Geophys. Res., 117, D04103, doi:10.1029/2011JD016620, 2012. 19509

Orr, J., Najjar, R., Sabine, C., and Joos, F.: Abiotic-how-to, Internal OCMIP Report, LSCE/CEA Saclay, 1999. 19504

Pierrehumbert, R.: Short-lived climate pollution, Annu. Rev. Earth Pl. Sc., 42, 341–379, doi:10.1146/annurev-earth-060313-054843, 2014. 19517

Schädel, C., Schuur, E. A., Bracho, R., Elberling, B., Knoblauch, C., Lee, H., Luo, Y., Shaver, G. R., and Turetsky, M. R.: Circumpolar assessment of permafrost C quality and its vulnerability over time using long-term incubation data, Glob. Change Biol., 20, 641–652, 2014. 19501, 19503, 19508, 19509, 19513, 19516, 19517

Schaefer, K., Zhang, T., Bruhwiler, L., and Barrett, A. P.: Amount and timing of permafrost carbon release in response to climate warming, Tellus B, 63, 165–180, doi:10.1111/j.1600-0889.2011.00527.x, 2011. 19501

Schaphoff, S., Heyder, U., Ostberg, S., Gerten, D., Heinke, J., and Lucht, W.: Contribution of permafrost soils to the global carbon budget, Environ. Res. Lett., 8, 014026, doi:10.1088/1748-9326/8/1/014026, 2013. 19501

Schmidt, M. W., Torn, M. S., Abiven, S., Dittmar, T., Guggenberger, G., Janssens, I. A., Kleber, M., Kögel-Knabner, I., Lehmann, J., Manning, D. A., Nannipieri, P., Rasse, D. P., Weiner, S., and Trumbore, S. E.: Persistence of soil organic matter as an ecosystem property, Nature, 478, 49–56, 2011. 19501, 19517

Schmittner, A., Oschlies, A., Matthews, H. D., and Galbraith, E. D.: Future changes in climate, ocean circulation, ecosystems, and biogeochemical cycling simulated for a business-as-usual CO_2 emission scenario until year 4000 AD, Global Biogeochem. Cy., 22, GB1013, doi:10.1029/2007GB002953, 2008. 19504

Schneider von Deimling, T., Meinshausen, M., Levermann, A., Huber, V., Frieler, K., Lawrence, D. M., and Brovkin, V.: Estimating the near-surface permafrost-carbon feedback on global warming, Biogeosciences, 9, 649–665, doi:10.5194/bg-9-649-2012, 2012. 19501

Schneider von Deimling, T., Grosse, G., Strauss, J., Schirrmeister, L., Morgenstern, A., Schaphoff, S., Meinshausen, M., and Boike, J.: Observation-based modelling of permafrost carbon fluxes with accounting for deep carbon deposits and thermokarst activity, Biogeosciences, 12, 3469–3488, doi:10.5194/bg-12-3469-2015, 2015. 19501, 19516, 19517

Scholes, R. and de Colstoun, E. B.: ISLSCP II Global gridded soil characteristics, available at: http://daac.ornl.gov/cgi-bin/dsviewer.pl?ds_id=1004, last access: 5 May 2011, 2012. 19504

Schuur, E., McGuire, A., Schädel, C., Grosse, G., Harden, J., Hayes, D., Hugelius, G., Koven, C., Kuhry, P., Lawrence, D., Natali, S. M., Olefeldt, D., Romanovsky, V. E., Schaefer, K., Turetsky, M. R., Treat, C. C., and Vonk, J. E.: Climate change and the permafrost carbon feedback, Nature, 520, 171–179, 2015. 19500, 19501, 19511, 19512, 19516, 19517

Schuur, E. A. G., Bockheim, J., Canadell, J. G., Euskirchen, E., Field, C. B., Goryachkin, S. V., Hagemann, S., Kuhry, P., Lafleur, P. M., Lee, H., Mazhitova, G., Nelson, F. E., Rinke, A., Romanovsky, V. E., Shiklomanov, N., Tarnocai, C., Venevsky, S., Vogel, J. G., and Zimov, S. A.: Vulnerability of permafrost carbon to climate change: implications for the global carbon cycle, BioScience, 58, 701–714, 2008. 19500, 19517

Serreze, M. C. and Barry, R. G.: Processes and impacts of Arctic amplification: a research synthesis, Global Planet. Change, 77, 85–96, 2011. 19509

Shiogama, H., Watanabe, M., Yoshimori, M., Yokohata, T., Ogura, T., Annan, J. D., Hargreaves, J. C., Abe, M., Kamae, Y., O'ishi, R., Nobui, R., Emori, S., Nozawa, T., Abe-Ouchi, A., and Kimoto, M.: Perturbed physics ensemble using the MIROC5 coupled atmosphere–ocean GCM without flux corrections: experimental design and results, Clim. Dynam., 39, 3041–3056, 2012. 19503, 19512

Smith, L.: Chaos: a Very Short Introduction, Oxford University Press, Oxford, UK, 2007. 19501, 19502

Steinacher, M., Joos, F., and Stocker, T. F.: Allowable carbon emissions lowered by multiple climate targets, Nature, 499, 197–201, 2013. 19502

Trumbore, S.: Age of soil organic matter and soil respiration: radiocarbon constraints on belowground C dynamics, Ecol. Appl., 10, 399–411, 2000. 19508, 19509

Weaver, A. J., Eby, M., Wiebe, E. C., Bitz, C. M., Duffy, P. B., Ewen, T. L., Fanning, A. F., Holland, M. M., MacFadyen, A., Matthews, H. D., Meissner, K. J., Saenko, O., Schmittner, A., Wang, H., and Yoshimori, M.: The UVic Earth System Climate Model: model description, climatology, and applications to past, present and future climates, Atmos. Ocean, 39, 1–67, 2001. 19503, 19504

Zhuang, Q., Melillo, J. M., Sarofim, M. C., Kicklighter, D. W., McGuire, D., Felzer, B. S., Sokolov, A., Prinn, R. G., Steudler, P. A., and Hu, S.: CO_2 and CH_4 exchanges between land ecosystems and the atmosphere in northern high latitudes over the 21st century, Geophys. Res. Lett., 33, L17403, doi:10.1029/2006GL026972, 2006. 19501

Zickfeld, K., Eby, M., Matthews, H. D., and Weaver, A. J.: Setting cumulative emissions targets to reduce the risk of dangerous climate change, P. Natl. Acad. Sci. USA, 106, 16129–16134, doi:10.1073/PNAS.0805800106, 2008. 19504

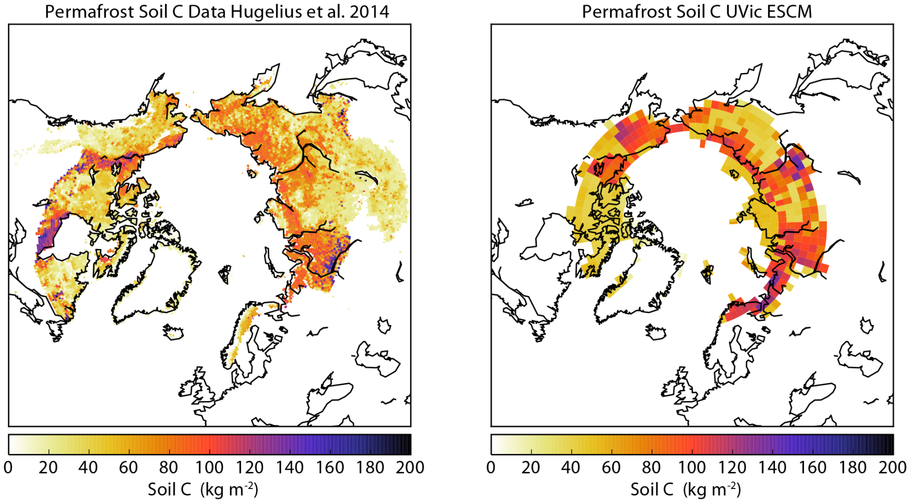

Figure 1. Comparison of the estimated soil carbon density in the top 3 m of soil in the Northern Hemisphere permafrost region from Hugelius et al. (2014) and soil carbon density in the top 3.35 m of soil in the permafrost region of the UVic ESCM. The model is able to capture the correct global total of soil carbon through tuning but with significant spatial biases.

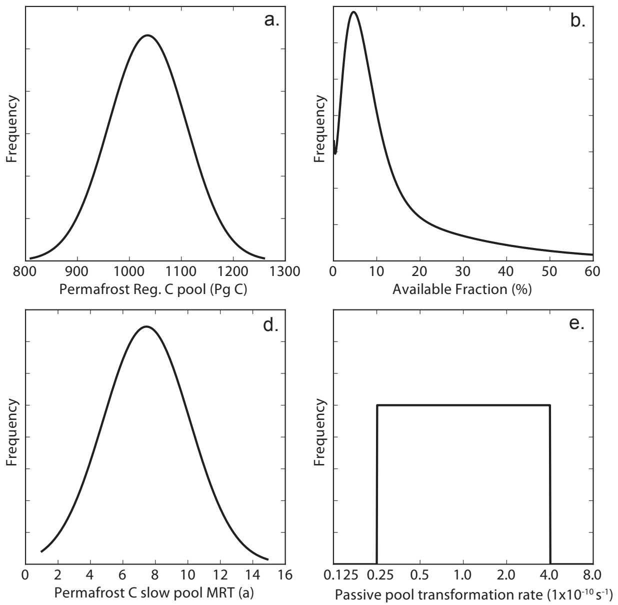

Figure 2. Probability distribution functions of the six parameters perturbed in this study. Panel **(b)** is the sum of three weighted gamma functions (one each for organic soil, shallow and deep mineral soil). Panel **(e)** has a logarithmic scale. MRT is mean residence time.

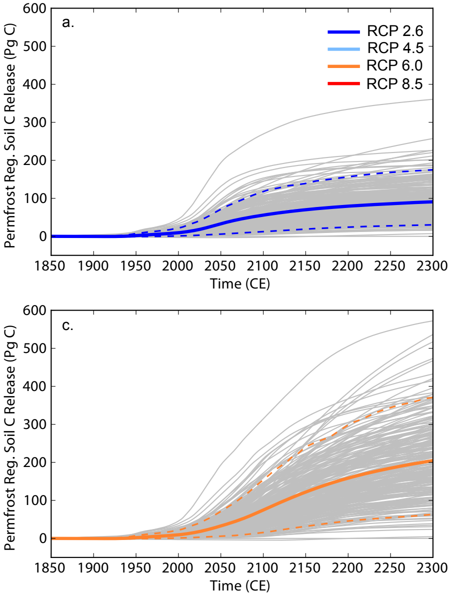

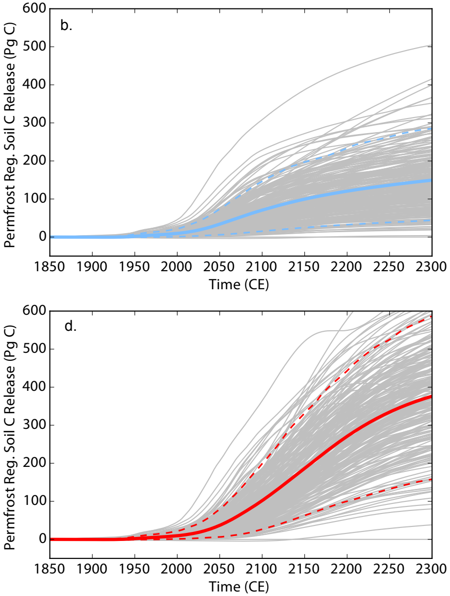

Figure 3. Release of carbon from the permafrost region for all 250 model variants (grey lines) and four RCP scenarios. Mean for each scenario shown with think solid line. Fifth and 95th percentiles shown with dashed lines.

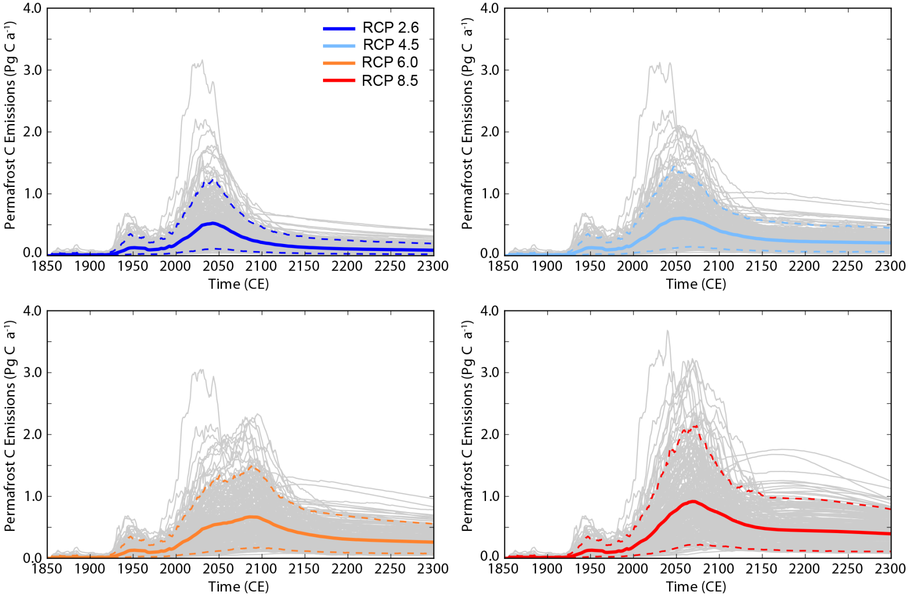

Figure 4. Emission of carbon from permafrost soils for each model variant (grey lines) and each RCP scenario. Mean for each scenario shown with think solid line. Fifth and 95th percentiles shown with dashed lines.

Title Page
Abstract | Introduction
Conclusions | References
Tables | Figures
◀| |▶
◀ ▶
Back | Close
Full Screen / Esc
Printer-friendly Version
Interactive Discussion

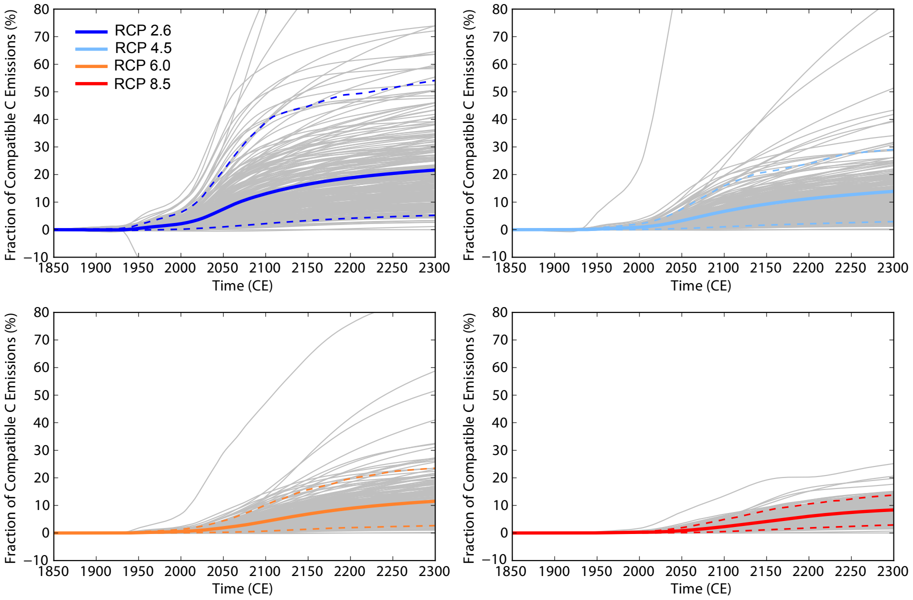

Figure 5. Cumulative emissions from permafrost soils relative to diagnosed compatible emissions for each model variant (grey lines) and each RCP scenario. Mean for each scenario shown with think solid line. Fifth and 95th percentiles shown with dashed lines. Note that under scenarios with lower emissions permafrost carbon emissions are larger relative to fossil fuel emissions.

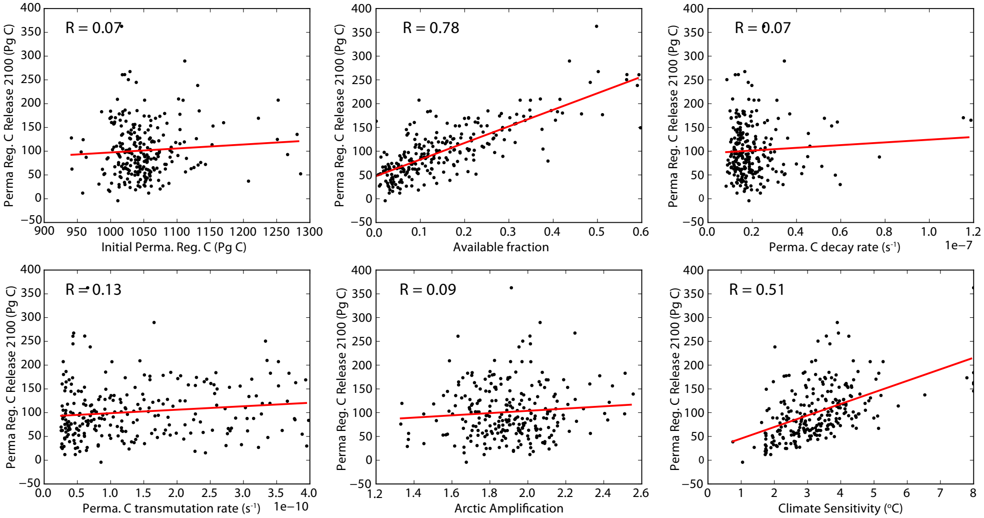

Figure 6. Correlation between release of carbon from the permafrost region in year 2100 under RCP 8.5 and value of perturbed model parameters. Red line is line of best fit and *R* is correlation coefficient.

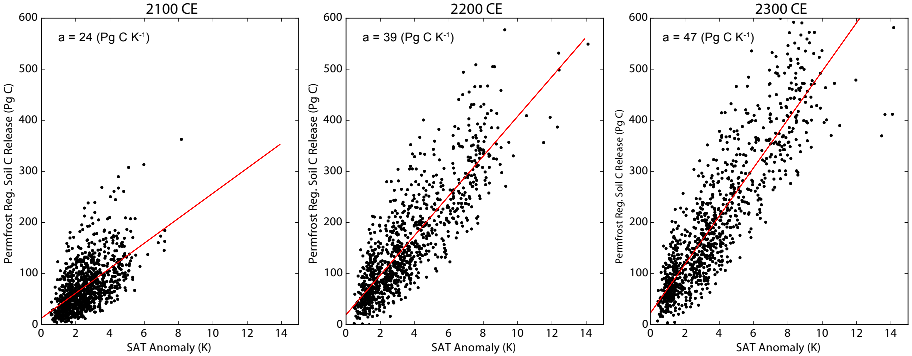

Figure 7. Correlation between release of carbon from the permafrost region and change in global temperature at years 2100, 2200, and 2300 CE. Red line is line of best fit and *a* is the slope of this line.

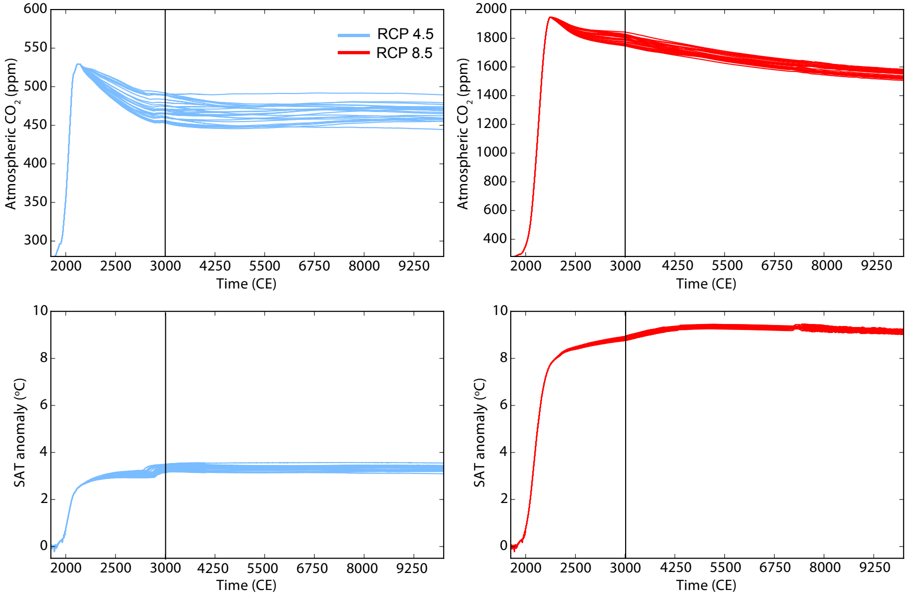

Figure 8. Evolution of CO_2 and surface air temperature (SAT) anomaly under continued RCPs 4.5 and 8.5 forcing until common era year 10 000. Vertical black line indicates change in horizontal scale.

Title Page
Abstract
Introduction
Conclusions
References
Tables
Figures
◀◀
▶▶
◀
▶
Back
Close
Full Screen / Esc
Printer-friendly Version
Interactive Discussion

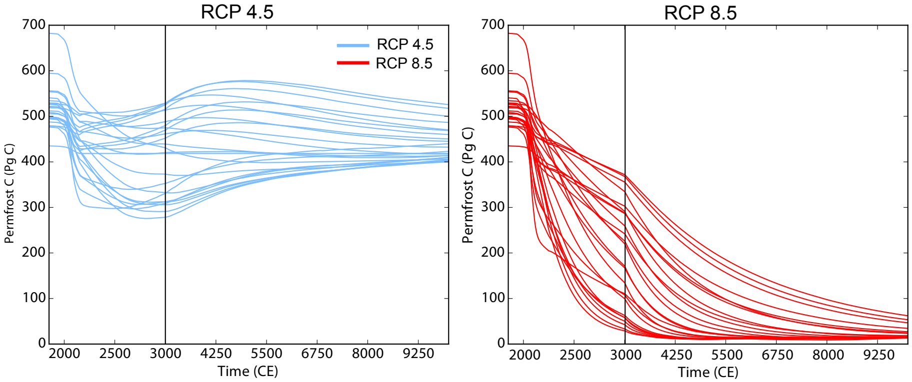

Figure 9. Evolution of permafrost soil carbon pool under continued RCPs 4.5 and 8.5 forcing until common era date 10 000. Vertical black line indicates change in horizontal scale. Under RCP 4.5 forcing the permafrost carbon pool undergoes a recovery in the late third millennium and under RCP 8.5 forcing declines toward a near zero value.

Title Page
Abstract
Introduction
Conclusions
References
Tables
Figures
|◀
▶|
◀
▶
Back
Close
Full Screen / Esc
Printer-friendly Version
Interactive Discussion

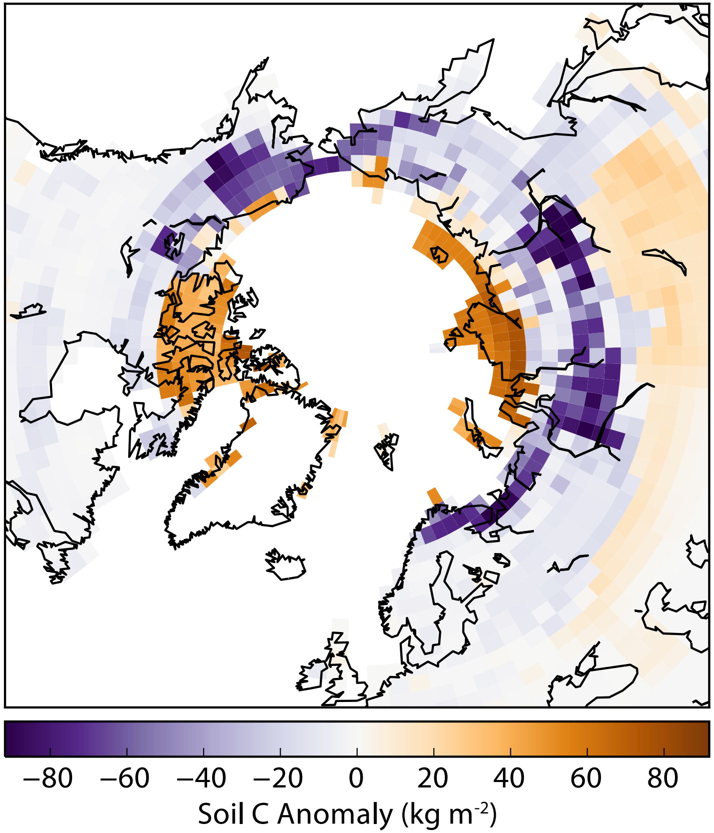

Figure 10. Difference between soil carbon density in Northern Hemisphere between 1875 and 5250 CE under continued RCP 4.5 forcing. A large permafrost carbon pool has developed in the high arctic by year 5250.